Desalination and Water Treatment
www.deswater.com

doi:10.5004/dwt.2019.23461

141 (2019) 95–105
February

Preparation of poly(vinylidene fluoride) (PVDF)/dopamine-modified sodium montmorillonite (D-MMT) composite membrane with the enhanced permeability and the mechanical property

Ying Cai[a], Jian Lu[a,*], Jun Wu[b]

[a]*Key Laboratory of Coastal Environmental Processes and Ecological Remediation, Yantai Institute of Coastal Zone Research, Chinese Academy of Sciences, Yantai, Shandong 264003,China, Tel. +86-535-2109278, Fax +86-535-2109000, email: jlu@yic.ac.cn (J. Lu)*
[b]*Qinghai Institute of Salt Lakes, Chinese Academy of Sciences, Xining, Qinghai 810008, China*

Received 30 June 2018; Accepted 12 November 2018

ABSTRACT

Dopamine modified sodium montmorillonite (D-MMT) was firstly used as the inorganic filler of polyvinylidene fluoride (PVDF) composite membranes via nonsolvent induced phase separation (NIPS) method. The surface modification sodium-montmorillonite (Na-MMT) was characterized by Fourier transform infrared (FTIR), thermo gravimetric analysis (TGA), X-ray diffraction (XRD) and transmission electron microscopy (TEM). The X-ray photoelectron spectroscopic (XPS) spectra and elemental mapping demonstrated that the D-MMT was incorporation and uniformly dispersed into PVDF composite membranes. Results showed that the incorporation of D-MMT into PVDF composite membranes significantly improved the mechanical property and hydrophilicity at a low D-MMT loading. The addition of 0.8 wt% D-MMT not only altered the morphology and structure of membranes, but also drastically increased tensile strength from 1.98 to 2.63 Mpa while elongation at break increased from 58% to 126%. In addition, the pure water flux of membranes increased by almost 50% from 15 to 22 L $m^{-2} h^{-1}$ when 0.8 wt% D-MMT was added. These results suggested that the surface modification of Na-MMT played an important role inimproving mechanical properties and pure water flux of PVDF composite membranes.

Keywords: Polyvinylidene fluoride; Composite membranes; Surface modification; Nonsolvent induced phase separation

1. Introduction

Polyvinylidene fluoride (PVDF) is widely used for various membranes. Although PVDF membranes have many advantages, a critical problem is the low mechanical strength of the membranes. The PVDF possesses the excellent chemical resistance, ability to maintain oxidative treatment, and film-forming properties so as to be widely used for various membrane industrial departments [1–3]. PVDF resin has a relatively low melting point of about 172°C and can be easily dissolved in many organic solvents such as dimethylacetamide (DMAc), dimethyl sulfoxide (DMSO), N,N-dimethylformamide (DMF) and so on [4,5]. PVDF membranes can be prepared by both nonsolvent-induced phase separation (NIPS) and thermally induced phase separation (TIPS) methods [6,7]. Although PVDF membranes have many advantages, various problems in a long-term application frequently occur. A critical problem in water treatment applications is the nearly inevitable issues on the mechanical strength of membranes. Under a high flow rate and operating pressure, the suspended coarse particles and other matters in the wastewater abrade and compact the membrane surface during filtration processes. Therefore, high-strength membranes are more likely to extend the service life of membrane modules [8].

*Corresponding author.

Several approaches have been conducted to explore the possibility of improving the mechanical and chemical properties of PVDF membranes [8–10]. Mixing organic and inorganic fillers in the PVDF casting solution is one of the popular modification methods because of its significant simplicity and effective improvement on performance characteristics of membranes such as the strength and pure water flux [11,12]. Special additives such as layered silicates (e.g., montmorillonite clay) have been in widespread use for PVDF composite membranes for decades [5,13] due to their excellent properties such as large diameter-thickness ratio, high stiffness, and huge specific surface area [14]. Different PVDF composite membranes with excellent performance can be easily prepared [15]. However, the inorganic components in the composite membranes tend to agglomerate because of their high surface energy [16,17]. The greater difference between PVDF polymer and inorganic materials makes the clay be easier to agglomerate. The membrane mechanical strength will decrease when a large number of additives in the composite membrane agglomerate [18].

Surface modifications of nanoparticles are often used to improve the mechanical and other performances of polymers [19,20]. A biomimetic synthetic polymer polydopamine (PDOPA), which can be easily achieved and possesses outstanding adhesion properties, has recently drawn extensive attention as a general surface modification agent with extremely good application potential [21–23]. Surface modification of sodium montmorillonite clay using dopamine can be prepared using a simple water-assisted process [24]. The incorporation of dopamine-modified clay (D-clay) extremely promotes the mechanical strength and other properties of epoxy resin [24], polyether polyurethane (PU) [25], polypropylene (PP) [26], and styrene butadiene rubber (SBR) [27]. The surface modification of the MMT not only effectively prevents D-clay aggregation but also improves its dispersion in the polymer. The great interfacial interactions of the D-clay in the epoxy leads to a good dispersion and significant increase in the stress transfer [24]. The mechanical properties of composites largely depend on stress transfer of matrix, thus resulting in significant improvements of mechanical properties at relatively low D-clay loadings. Sodium montmorillonite clay (Na-MMT) was used by this study due to its hydrophilicity, low price, and high stiffness. Dopamine-modified Na-MMT (D-MMT) was used as the inorganic filler in order to produce reinforced PVDF ultrafiltration composite membranes via NIPS method. This study investigated the chemical, mechanical, thermal, and hydrophilicity properties of the PVDF membranes reinforced by D-MMT. This study attempts to obtain the initial information on the improvement of PVDF composite membrane using D-MMT, which can provide new direction on low-price, easy-preparation, and effective composite membranes.

2. Materials and methods

2.1. Materials

PVDF (Mn = 110,000 g/mol, Solef 6010) used in this study was purchased from Solvay Solexis (Belgium). Na-MMT was supplied by Zhejiang Fenghong Clay Chemicals Co, Ltd (Anji, China). PVDF and Na-MMT were desiccated at 110°C for one day before use. DMAc (analytical reagent grade) and polyvinylpyrrolidone (PVP, K30) were obtained from Sinopharm Chemical Reagent Co. (Beijing, China). Dopamine hydrochloride (DOPA) purchased from Shanghai Yuanye Biological Technology Co. (Shanghai, China) and bovine serum albumin (BSA, with molecular weight of 67,000 Da) obtained from Sigma-Aldrich Co. (St Louis, USA) were used without further processing. Tris–HCl (pH = 9.0) was obtained from Beijing Solarbio Science & Technology Co. (Beijing, China).

2.2. Preparation of D-MMT

Na-MMT (10 g) was dispersed in 200 mL of deionized water and mechanically stirred for 36 h followed by 1-h ultrasonic stirring. Then 0.5 g DOPA and 2 mM Tris-HCl were added and pH of the suspension was adjusted to 8.5 by using 1.0 M NaOH. After stirred at 300–400 rpm in room ambient environment for 6 h, the suspension was centrifuged at 4,000 rpm for 30 min. Isopropanol and acetone were used to wash the dark slurry-like product in turn, and then were removed by centrifugation. The process of washing and centrifugation was repeated at least 5 times. Finally the surface modification Na-MMT/acetone slurry was dried in an oven at about 60°C for 2 d to obtain D-MMT.

Polydopamine was prepared by the following steps similar with those of D-MMT. Dopamine was self-polymerized in Tris buffer for 6 h, and then the products were centrifuged at 4,000 rpm for 30 min. The dark slurry-like products were washed by isopropanol and acetone in turn. Finally the products were dried in an oven at about 60°C for 2 d.

2.3. Preparation of PVDF composite membranes

Nonsolvent-induced phase separation (NIPS) method was used to prepare PVDF composite membranes. D-MMT was ultrasonically dispersed in DMAc and then agitated for 24 h before adding PVDF and PVP powders. The casting solution was mechanically stirred at 40°C until the polymer was completed dissolved. Then the casting solution was placed in a vacuum dryer for 24 h for the sake of removing air bubbles. The PVDF solution was casted onto a glass plate with the casting thickness of about 200 μm using a casing knife at room temperature. Then the glass plate was immediately put into the water bath to form a PVDF membrane [28]. The compositions of these PVDF membranes were exhibited in Table 1.

2.4. Characterization of D-MMT

The Fourier transform infrared (FTIR) spectra of DOPA, PDOPA, Na-MMT and D-MMT were tested from 500 to 4000 cm^{-1} by a JASCO 4100 instrument (JASCO, Japan) at room temperature. The thermo gravimetric analysis (TGA) was conducted using a TA Instrument (Mettler 5MP). The samples were heated from room temperature to 850°C at 10°C min^{-1} in nitrogen. X-ray diffraction (XRD) spectra were determined on an X-ray powder diffractometer instrument

Table 1
The detailed composition of different membranes

Type of membrane	PVDF (wt%)	D-MMT (wt%)	PVP (wt%)	DMAc (wt%)
M0	15.0	0.0	1.0	84.0
M1	15.0	0.2	1.0	83.8
M2	15.0	0.4	1.0	83.6
M3	15.0	0.6	1.0	83.4
M4	15.0	0.8	1.0	83.2
M5	15.0	1.0	1.0	83.0
M6	15.0	1.5	1.0	82.5
M7	15.0	2.0	1.0	82.0
M8	15.0	2.5	1.0	81.5

(BRUKER D8 Advance, Bruker Corporation, Germany).The XRD pattern was scanned in 2θ range of 2–30°. The d-spacing can be calculated according to Bragg's law:

$$2d\sin\theta = n\lambda \tag{1}$$

where n is an integer and assumed to be 1; λ is the wavelength of the incident X-rays (Cu-Kα: λ = 0.15406 nm); 2θ is the diffraction angle [29,30]. The structure of the Na-MMT and D-MMT were also analyzed using transmission electron microscopy (TEM, FEI Tecnai G2 F20, FEI, USA).

2.5. Characterization of PVDF membranes

The wet membranes were used directly for flux and BSA rejection tests while they were freeze-dried prior to other characteristic tests. The X-ray photoelectron spectroscopic (XPS) measurements of membranes were obtained by an ESCALAB 250Xi (Thermo Scientific, USA) with using Al Kα X-ray as the excitation source (hv = 1486.6 eV). The morphologies of the membranes including top surface (water side) and cross section were measured by a field emission scanning electron microscope (SEM) (Hitachi S-4800, Hitachi Ltd, Japan). The cross-section images of PVDF membranes were acquired after being freeze-dried and fractured in liquid nitrogen. Moreover, elemental mapping of silicon and aluminum in the PVDF composite membranes was obtained using an Energy Dispersive Spectrometer (EDS) (Hitachi S-4800, Hitachi Ltd, Japan). Atomic force microscopy (AFM) MultiMode 8+Bioscope Catalyst (VEECO, USA) was used to obtain the top surface roughness. This measurement was operated at an area of 10 μm × 10 μm.

The tensile strength and elongation of PVDF membrane at the breaking point were determined using a tensile machine (HY0580, Shanghai Hengyi Testing Machine Co., Ltd., China) at a speed of 1 mm min^{-1} and the maximum load of 10 N. Each membrane was measured at least 5 times and the average value with deviation was reported. The water contact angle (CA) was measured by a contact angle analyzer (OCA50, Dataphysics, Germany) to explore the surface hydrophilicity of the PVDF membranes. 2 μL of DI water droplets were dropped onto the top surface of PVDF membrane samples at ambient temperature. At least five experimental data at different sites of each PVDF membrane were acquired and the mean value was obtained. The filtration performance was tested using a dead-end stirred cell (Model 8010, Amicon Corp., USA). The stirred cell with a 25 mm diameter was connected to a nitrogen-pressurized solution reservoir. In each test, PVDF membrane samples were tested at 0.15 Mpa for 30 min and then measured at 0.1 Mpa for 30 min using DI water at 25°C. The pure water flux (PWF) was computed according to the below equation:

$$J_w = \frac{Q}{A\cdot\Delta T} \tag{2}$$

where J_w is the pure water flux (PWF, L m^{-2} h^{-1}); Q is volume of the permeated pure water (L); A is the effective filtration membrane area (m^2); ΔT is the permeation time (h). BSA rejection of the PVDF membrane was tested at 0.1 MPa and 25°C. BSA with concentration of 1 g L^{-1} was dissolved in phosphate buffer saline (PBS) solution (pH 7.4). BSA rejection (R) was calculated as Eq. (3).

$$R(\%) = \left(1-\frac{C_p}{C_0}\right)\times 100 \tag{3}$$

where C_p and C_0 are the concentration of protein in the permeation and the feed solution, respectively. The BSA concentration was tested using aTU-1810 spectrophotometer (Puxi Analytic Instrument Ltd., Beijing, China) at wavelength of 280 nm.

3. Results and discussion

3.1. Characterization of D-MMT

3.1.1. FTIR and TGA analysis

The FTIR and TGA curves of DOPA, PDOPA, Na-MMT and D-MMT are shown in Fig. 1. Many narrow peaks of DOPA were the characteristics of a small molecule [31] (Fig. 1A). The peaks at around 1504 cm^{-1} represented the asymmetric stretching vibrations of N–H from amino-group. The peaks at 3348 cm^{-1} represented the stretching vibrations of N–H [29]. PDOPA had characteristic bands around 1618 cm^{-1} representing aromatic rings and around 3359 cm^{-1} referring to catechol –OH groups [32] while Na-MMT had characteristic bands O–H (3428 cm^{-1}). The bands at 1639 cm^{-1} according to the H–O–H bond of water molecules retained in the silica matrix. The spectral band at 1037 cm^{-1} represented the Si–O–Si bond of the SiO_2 [29]. After surface modification using dopamine,the intensity of two peaks at around 1618 cm^{-1} and 3359 cm^{-1} increased, which indicates the incorporation of PDOPA in Na-MMT. Typical TGA curves of the DOPA, PDOPA, MMT, and D-MMT are shown in Fig. 1 B. Pure Na-MMT exhibited excellent thermo-stability with a residue as high as about 92% at 800°C. PDOPA started to decompose at less than 230°C [24]. The weight loss decreased to about 70% when the temperature increased to 800°C, which could be attributed to the degradation of PDOPA [31]. For D-MMT, the weight loss was lower than that of the pure Na-MMT, which was attributed to the decomposition of PDOPA in the structure of D-MMT. The TGA curves demonstrated that the PDOPA was coated on the NA-MMT.

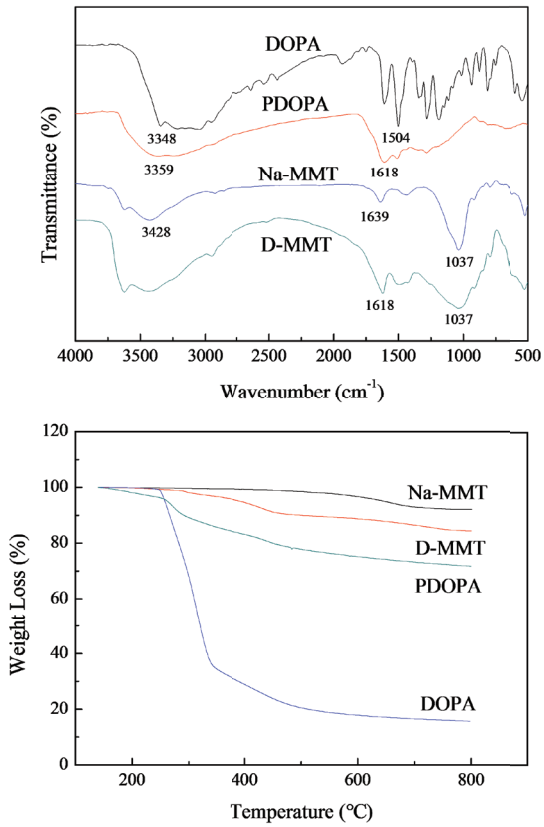

Fig. 1. Fourier transform infrared (FTIR) and thermo gravimetric analysis (TGA) curves of dopamine (DOPA), polydopamine (PDOPA), sodium montmorillonite clay (Na-MMT) and dopamine-modified sodium montmorillonite clay(D-MMT).

3.1.2. XRD measurement for D-MMT

The XRD patterns of D-MMT and Na-MMT are compared in Fig. 2. Na-MMT showed the 001 peak at 2θ = 7.20°. The interlayer d-spacing of Na-MMT was calculated to be 1.23 nm according Eq. (3) [33,34]. The D-MMT showed a narrow peak at 2θ = 6.75° after polymerization for 6 h, which corresponded to d-spacing of 1.31 nm [34,35]. This could be concluded that the distance of Na-MMT sheets is expanded by the PDOPA, which would provide better dispersion and stability in PVDF membranes [30].

3.1.3. TEM images of D-MMT

Both TEM images of the pristine Na-MMT and D-MMT illustrated that the products had a layered structure (Fig. 3). After modification, the particles became smaller and less coalescent. The surface energy of the Na-MMT decreased owing to modification. These features improved the dispersion property and thus prevented the agglomeration of particles.

3.2. Characterization of PVDFcomposite membranes

3.2.1. XPS analysis of PVDF composite membranes

The elemental compositions of the composite membranes M0 and M4 are shown in Fig. 4. Peaks of carbon

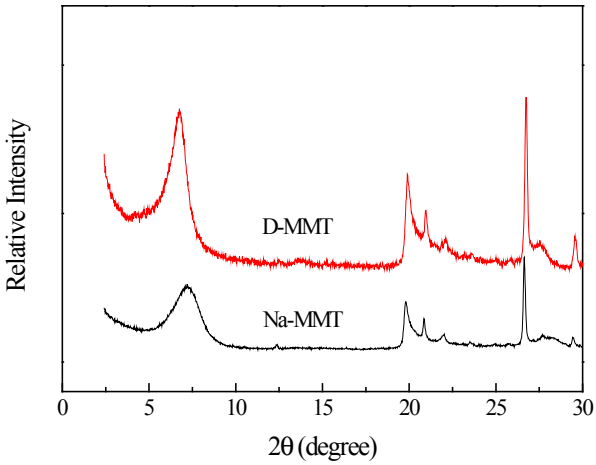

Fig. 2. X-ray diffraction (XRD)patterns of Na-MMT and D-MMT.

(binding energy, 295.38 eV), N1s (binding energy, 399.08 eV), O1s (binding energy, 541.78 eV) and F1s (binding energy, 687.08 eV) were observed on the surfaces of pristine and composite PVDF membranes [36–38]. Compared to the pristine PVDF membrane, the intensity of O1s drastically increased in the composite membrane, which was ascribed to the presence of Al_2O_3/SiO_2 on membrane surface (Fig. 4A). Moreover, the peak of Si2p (Fig. 4B) locating at 108.08 eV further confirmed the appearance of Si element [39].

3.2.2. Morphology of PVDF composite membranes

The surface and cross section images of the PVDF membrane are shown in Fig. 5 and Fig. 6, respectively. The membranes had an asymmetric structure with a thin and dense top surface layer as well as a bi-continuously interconnected support layer. This was produced by the fast exchange between solvent and nonsolvent [40,41]. For the pristine PVDF membranes, the interaction between solvent DMAc and water resulted in liquid-liquid separation to form a thin and dense skin structure on the top surface of the PVDF membrane and a macroviod structure in the membrane sublayer [42]. For the composite membranes, the mass transfer rate between casting solution surface and water increased due to the presence of hydrophilic D-MMT to thus form the loose upper surface with large pore structure [43,44]. The large pores on the membrane surface increased with the increase in D-MMT content, which could be explained by that D-MMT could promote phase inversion as pore-forming agent during membrane formation [45]. The sublayer of the composite membranes gradually changed from macroviod structure to spongy like structure. The elemental mapping was used to study the dispersion of D-MMT on top surface of M4 and M8 in the membrane (Fig. 7). The elementals silicon and aluminum were introduced by D-MMT and evenly distributed on the surface of M4. These results proved that D-MMT was well dispersed in the PVDF membrane. Excessive particles led to uneven dispersion and thus formed agglomeration (M8) as the concentration of D-MMT increased. These results indicate that the surface modification of Na-MMT

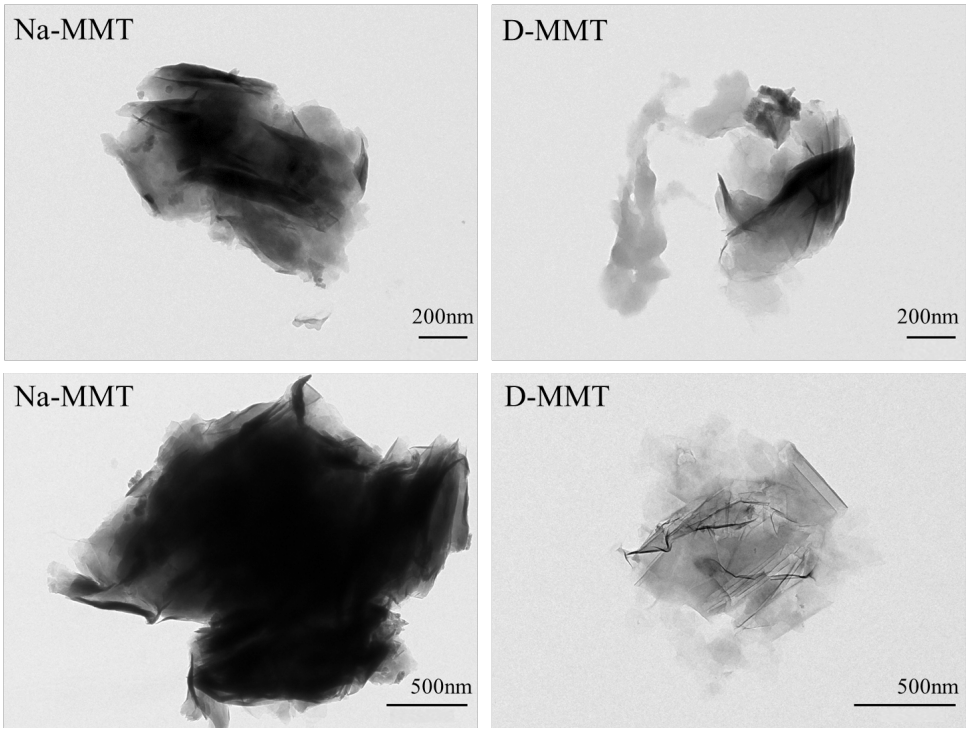

Fig. 3. Transmission electron microscopy (TEM) micrographs of Na-MMT and D-MMT particles.

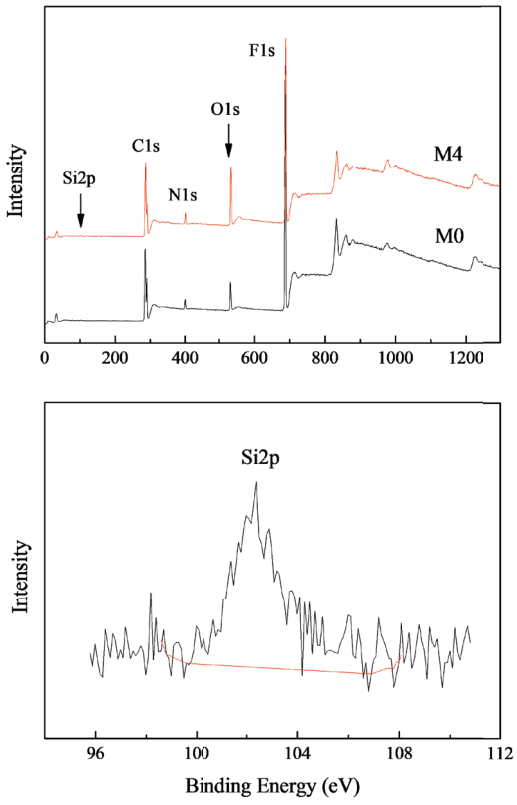

Fig. 4. X-ray photoelectron spectroscopic (XPS) spectra of PVDF and composite membrane M4: (A) wide survey XPS spectra, (B) Si2p XPS spectra of PVDF composite membrane; (C) Al2p XPS spectra of PVDF composite membrane.

significantly benefited the intercalation of D-MMT in PVDF membrane because of its stronger interactions with the matrix [24]. The surface roughness of various membranes is illustrated by Fig. 8. The mean surface roughness of pure PVDF membrane was 13 nm and increased as the D-MMT was added. The surface roughness of D-MMT membrane increased to 28.8 nm when the concentration of D-MMT was up to 2.5 wt% (M8). This result was in agreement with that of the SEM analysis. The dense membrane surface had a relative low surface roughness while a loose upper with large pore structure membrane surface had a higher surface roughness. The surface roughness increased with the increase of membrane pores.

3.2.3. Performance of PVDF composite membranes

To demonstrate the reinforcement of D-MMT on mechanical properties of PVDF membranes, the tensile strength and elongation at break were tested (Fig. 9). It could be seen that PVDF membranes containing D-MMT exhibited higher tensile strength and elongation at breaking than pristine PVDF membrane. The tensile strength and elongation at break increased firstly until reached the maximum values with D-MMT addition of 0.8 wt% (M4). The tensile strength of PVDF membrane was 1.98 MPa while it increased to 2.63 MPa with almost 33% of improvement through incorporation of a few of D-MMT (0.8 wt%). Meanwhile, the elongation increased from 58% to 126%. The sharp increase in the tensile strength and elongation could be primarily attributed to the effective load transfer offered by the D-MMT interface [26]. The crosslinking behavior of the D-MMT particles caused high mechanical properties [46,47]. In addition, the high mechanical prop-

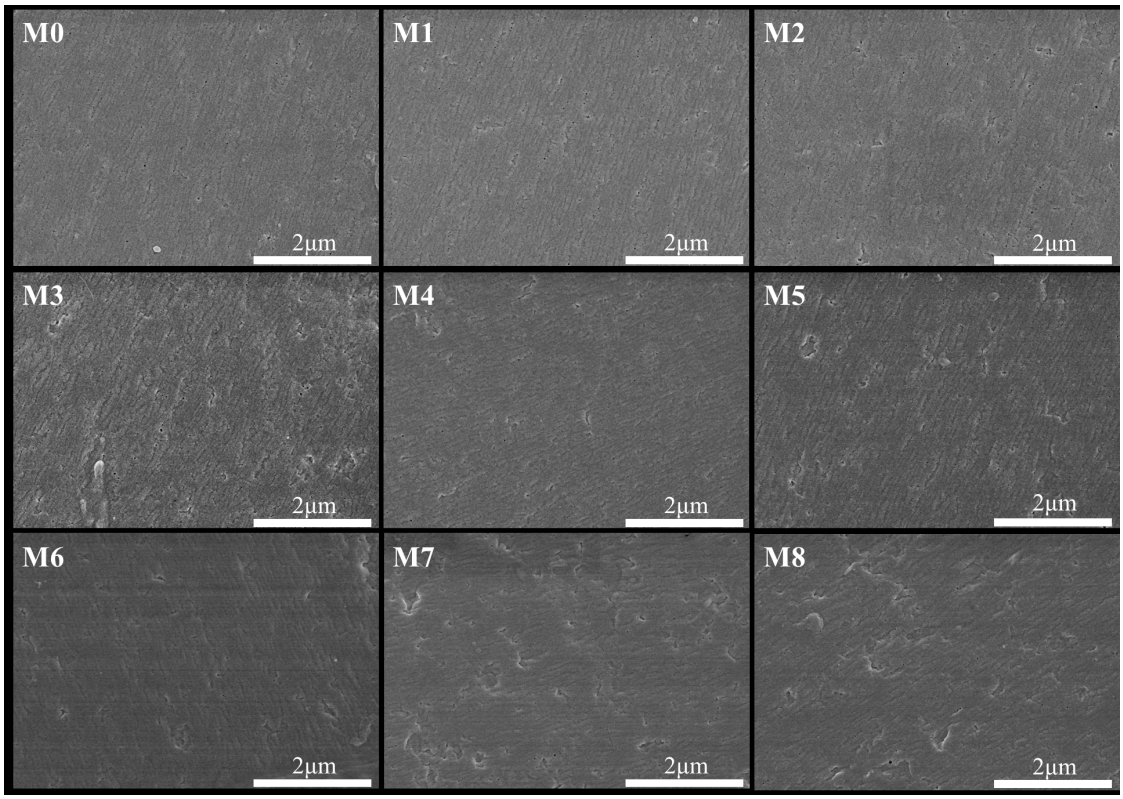

Fig. 5. Surface scanning electron microscope (SEM) images of M0–M8 membranes.

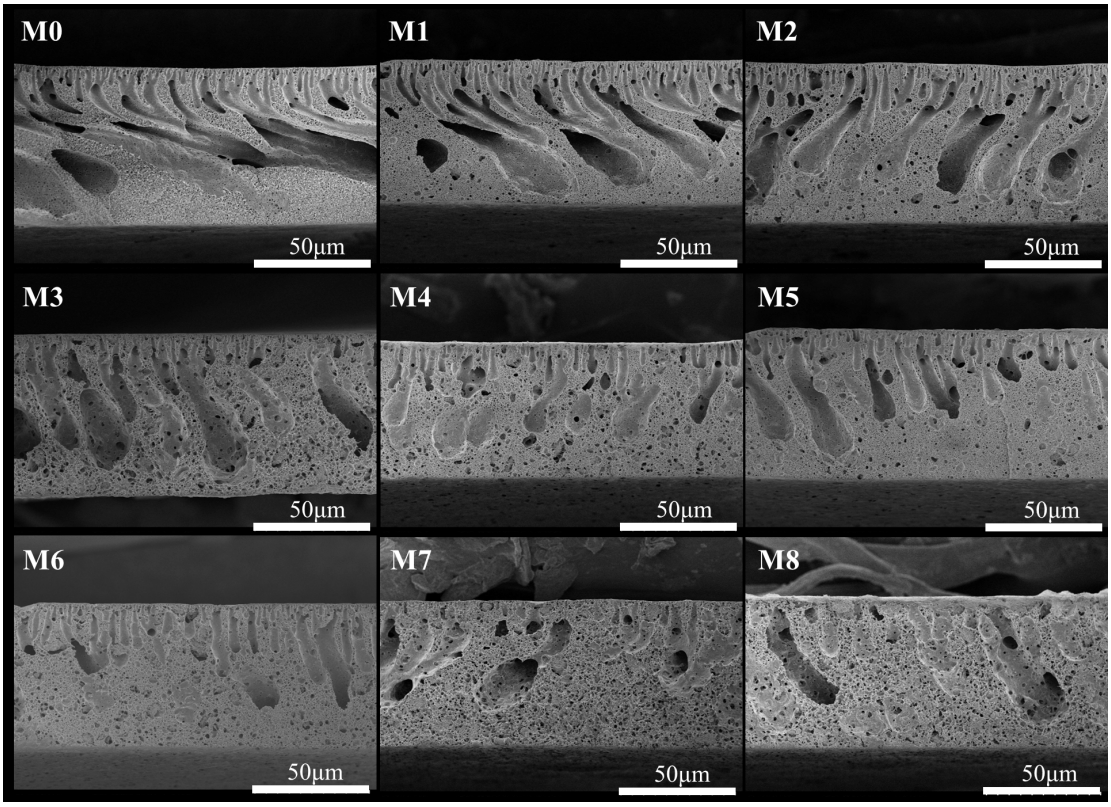

Fig. 6. Cross-section scanning electron microscope (SEM) images of membranes M0 to M8.

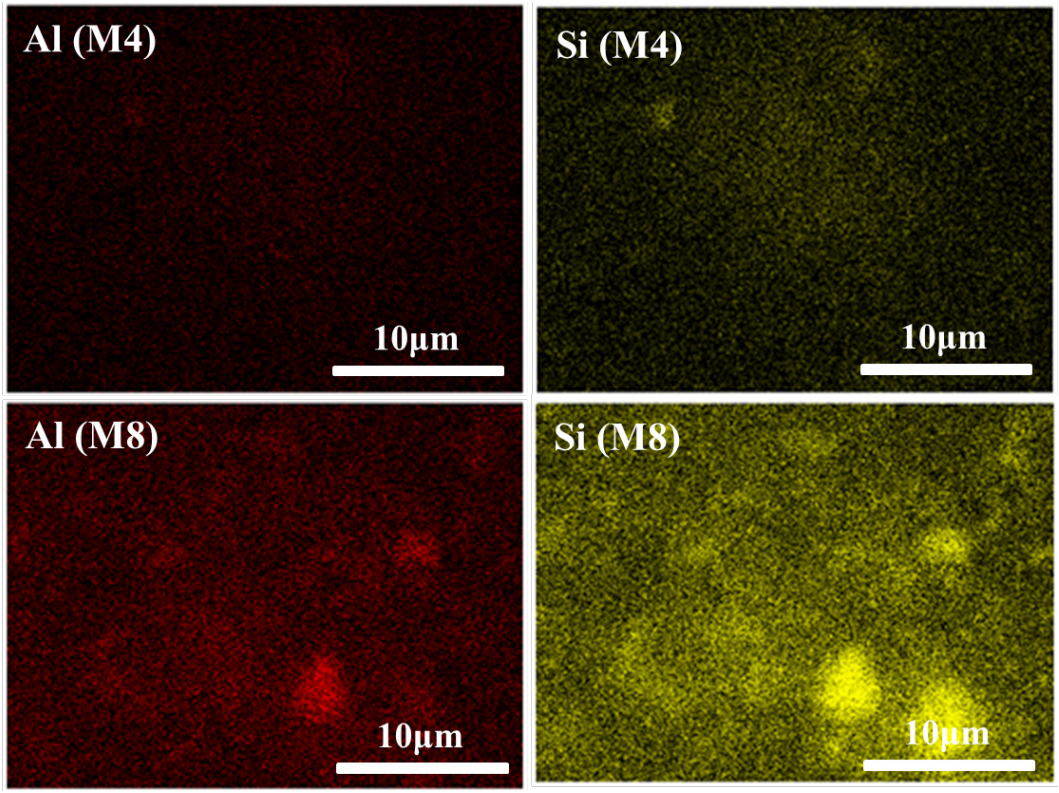

Fig. 7. Energy Dispersive Spectrometer (EDS) elemental mapping of the surface of PVDF composite membranes M4 and M8.

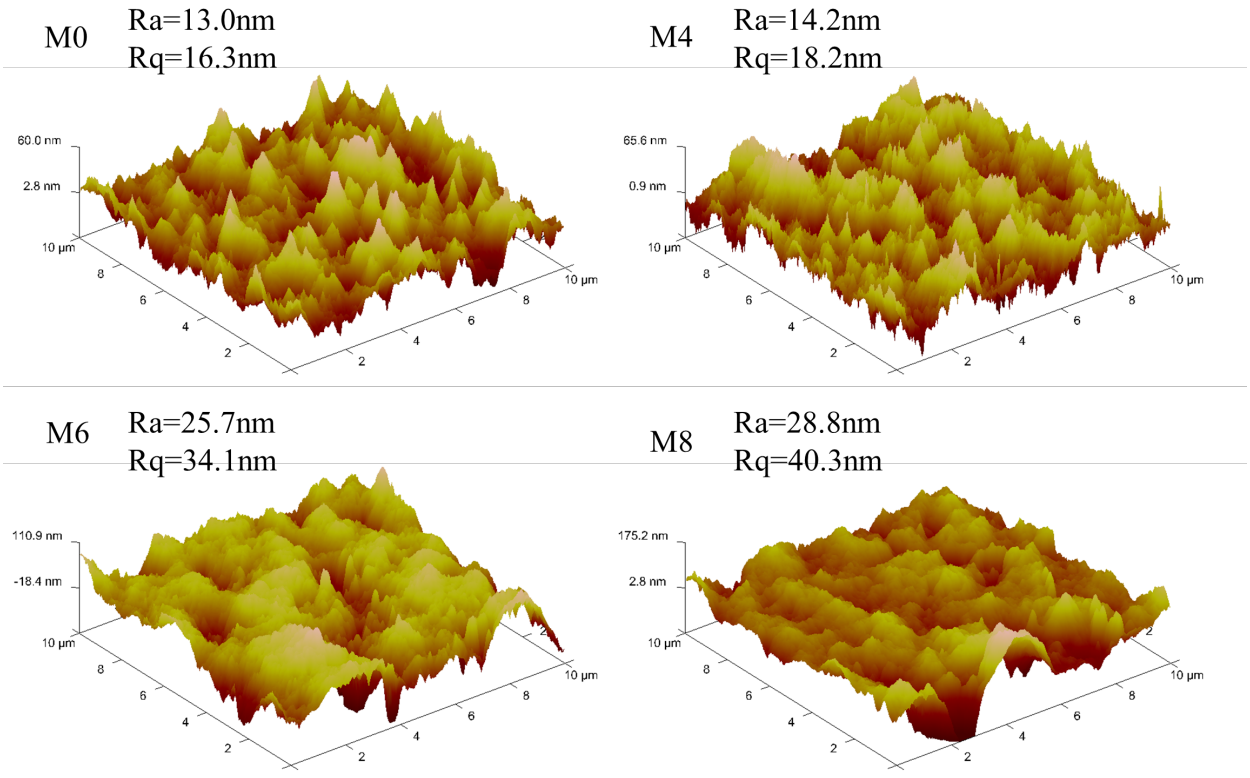

Fig. 8. Atomic force microscopy (AFM) images (10 μm × 10 μm) of membrane surface M0, M4, M6 and M8.

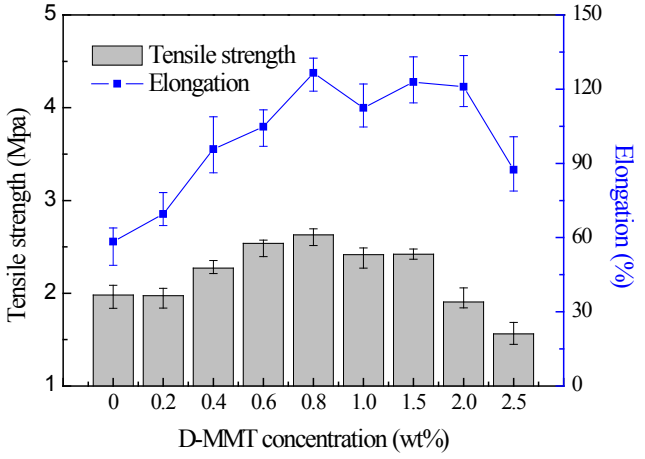

Fig. 9. Tensile strength and elongation of PVDF composite membranes with different D-MMT concentration.

erties could also be explained by morphological results of membranes. The macrovoid structure gradually turned into sponge-like structure when the D-MMT particles were incorporated in the membranes. Membranes with a sponge-like morphology have superior mechanical properties according to the literatures [48–50]. These results were in good agreement with the previous theoretical and experimental studies [25,26]. Agglomeration occurred when D-MMT composition continued to increase. The uneven distribution of particles produced large pores and some defected in the PVDF composite membranes, which caused degradation of mechanical properties.

The hydrophilicity of membranes is shown in Fig. 10. All the water contact angles of membranes were around 75° (Fig. 10A). Due to the hydrophilic of Na-MMT and PDOPA, the water contact angle of the membrane dropped slightly from 74.5° (M0) to 73.5° (M4) with the content increase of D-MMT, indicating that the hydrophilicity of membranes increased. As the D-MMT incorporation further increased to 2.5 wt% (M8), the water contact angle of membranes increased conversely due to the particle agglomeration [51]. Pure water flux (PWF) and BSA rejection were tested for all of the composite membranes (Fig. 10B). The incorporation of the D-MMT altered the surface hydrophilicity properties of PVDF to increase the filtration properties. In addition, the quantities of big cavities increased with the addition of D-MMT, which could lead to the enhancement of purewater flux [52]. A sharp increase of PWF from 15to 22 L $m^{-2}h^{-1}$ was observed in Sample M0 (0 wt% D-MMT) to Sample M4 (0.8 wt% D-MMT). This result was consistent with SEM and CA results. The incorporation of hydrophilic D-MMT caused a decrease in BSA rejection from 90% to 53% because of the increased big cavities on top surface which were proved by SEM and AFM. With the further increase of D-MMT content, the hydrophilicity of membrane surface decreased due to the agglomeration of the D-MMT, which subsequently led to the decrease in the pure water flux. The addition of D-MMT might be a promising modification approach for PVDF membrane because of low cost, fine accessibility of MMT, and the sharp increase in the water flux and rejection using D-MMT.

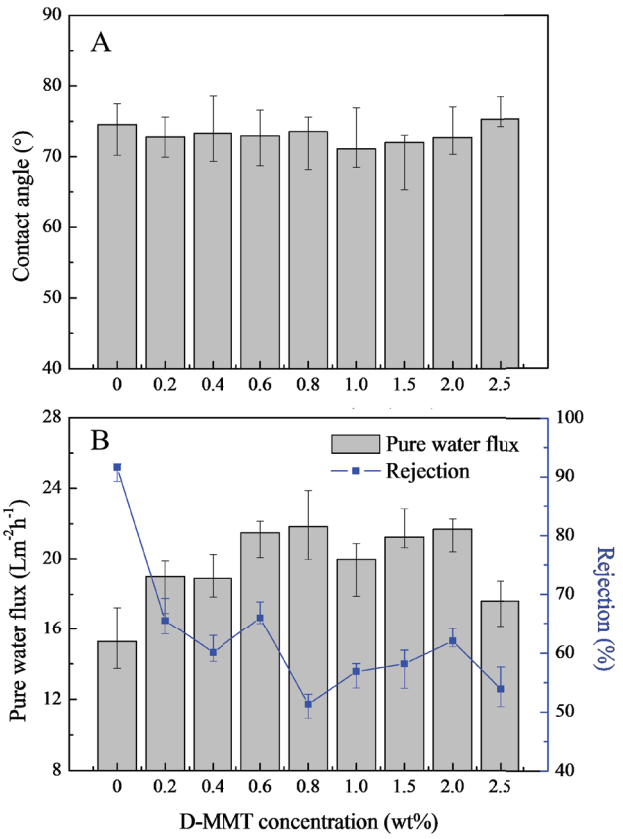

Fig. 10. Contact angle (A), pure water flux and rejection (B) of PVDF composite membranes in different D-MMT concentration.

3.2.4. Comparison of the performance of PVDF membranes modified by clay and dopamine modified clay

The flux and mechanical properties of PVDF hybrid membranes with the data obtained from previous literature and our work are shown in Table 2. Compared with other PVDF membranes added with unmodified clay, our membranes used the less content of dopamine modified Na-MMT to make the performance of membrane be improved greatly. The incorporation of D-MMT not only improved the hydrophilicity and permeability of the hybrid membranes, but also enhanced the tensile strength and elongation at break. The results show that D-MMT has provided new opportunities for improving the mechanical properties and pure water flux of PVDF membranes.

4. Conclusions

Dopamine modified sodium montmorillonite clay was firstly used as the inorganic filler of PVDF composite membranes via NIPS method. The Fourier transform infrared (FTIR), thermo gravimetric analysis (TGA) and X-ray diffraction (XRD) tests proved that Na-MMT was successfully modified by dopamine. The X-ray photoelectron spectroscopic (XPS) spectra and elemental mapping demonstrated that the D-MMT was incorporation and uniformly dispersed into PVDF composite mem-

Table 2
The detailed composition of different membranes

Fillers	Optimum dosage of fillers (wt%)	Rate of change in water flux (%)	Rate of change in tensile strength (%)	Rate of change in elongation at break (%)	Reference
Palygorskite	10	↑35	↑16.7	↓-38.4	[8]
Clay	1	↑113	–	↓-20	[13]
MMT	5	↑38	–	–	[53]
Cloisite 30B	5.08	↓-37.4	↑13.7	↓-8	[54]
Nanomers 1.44P	5.08	↓-6.5	↑1.6	↓–30.9	[54]
MMT	5	↑37.5	↑23.3	↓–50	[55]
Nanoclay	5	–	↑8.1	↑100	[56]
D-A-HNTs	0.36	↑82.6	–	–	[17]
D-MMT	0.8	↑46.7	↑33	↑117	This work

branes. The incorporation of D-MMT played an important role during the phase separation process. Compared with other PVDF membranes added with unmodified clay, composite membranes with a small amount D-MMT had higher breaking strength and elongation at break. The presence of D-MMT also increased the pure water flux of the PVDF membrane, making the PVDF/D-MMT composite membrane a good membrane candidate for wastewater treatment.

Acknowledgements

This study was funded by the National Natural Science Foundation of China (Nos.41671319 and 41877131), One Hundred Talents Program of Chinese Academy of Sciences (No. Y629041021 and Y610061033), Taishan Scholar Program of Shandong Province, Natural Science Foundation of Shandong Province (No. ZR2014BQ005), Key Research Program of Frontier Sciences of CAS (Grant No.QYZDJ-SSW-DQC015), and Two Hundred Talents Program of Yantai (No.Y739011021). The authors would like to thank the reviewers for their valuable suggestions and comments on the manuscript.

Conflict of Interest

The authors declare that they have no conflict of interest.

References

[1] L.M. Corneal, M.J. Baumann, S.J. Masten, S.H.R. Davies, V.V. Tarabara, S. Byun, Mn oxide coated catalytic membranes for hybrid ozonation-membrane filtration: Membrane microstructural characterization, J. Membr. Sci., 369 (2011) 182–187.
[2] C. Sun, X. Feng, Enhancing the performance of PVDF membranes by hydrophilic surface modification via amine treatment, Sep. Purif. Technol., 185 (2017) 94–102.
[3] X. Yang, Y. He, G.Y. Zeng, Y.Q. Zhan, Y. Pan, H. Shi, Q. Chen, Novel hydrophilic PVDF ultrafiltration membranes based on a ZrO_2-multiwalled carbon nanotube hybrid for oil/water separation, J. Mater. Sci., 51 (2016) 8965–8976.
[4] Y. Subasi, B. Cicek, Recent advances in hydrophilic modification of PVDF ultrafiltration membranes – a review: part I, Membr. Technol., 2017 (2017) 7–12.
[5] G. Kang, Y. Cao, Application and modification of poly(vinylidene fluoride) (PVDF) membranes – A review, J. Membr. Sci., 463 (2014) 145–165.
[6] J.F. Kim, J.T. Jung, H.H. Wang, S.Y. Lee, T. Moore, A. Sanguineti, E. Drioli, Y.M. Lee, Microporous PVDF membranes via thermally induced phase separation (TIPS) and stretching methods, J. Membr. Sci., 509 (2016) 94–104.
[7] W.C. Chong, E. Mahmoudi, Y.T. Chung, M.M. Ba-Abbad, C.H. Koo, A.W. Mohammad, Polyvinylidene fluoride membranes with enhanced antibacterial and low fouling properties by incorporating ZnO/rGO composites, Desal. Water Treat., 96 (2017) 12–21.
[8] J. Ji, S. Zhou, C.Y. Lai, B. Wang, K. Li, PVDF/palygorskite composite ultrafiltration membranes with enhanced abrasion resistance and flux, J. Membr. Sci., 495 (2015) 91–100.
[9] A. Jafari, M.R.S. Kebria, A. Rahimpour, G. Bakeri, Graphene quantum dots modified polyvinylidenefluride (PVDF) nanofibrous membranes with enhanced performance for air Gap membrane distillation, Chem. Eng. Process., 126 (2018) 222–231.
[10] A.L. Ahmad, U.R. Farooqui, N.A. Hamid, Effect of graphene oxide (GO) on Poly(vinylidene fluoride-hexafluoropropylene) (PVDF-HFP) polymer electrolyte membrane, Polymer, 142 (2018) 330–336.
[11] X. Wu, B. Zhao, L. Wang, Z. Zhang, H. Zhang, X. Zhao, X. Guo, Hydrophobic PVDF/graphene hybrid membrane for CO_2 absorption in membrane contactor, J. Membr. Sci., 520 (2016) 120–129.
[12] P.S. Goh, A.F. Ismail, A review on inorganic membranes for desalination and wastewater treatment, Desalination, 434 (2018) 60–80.
[13] M.H.D.A. Farahani, V. Vatanpour, A comprehensive study on the performance and antifouling enhancement of the PVDF mixed matrix membranes by embedding different nanoparticulates: Clay, functionalized carbon nanotube, SiO_2 and TiO_2, Sep. Purif. Technol., 197 (2018) 372–381.
[14] P. Anadão, L.F. Sato, R.R. Montes, H.S. De Santis, Polysulphone/montmorillonite nanocomposite membranes: Effect of clay addition and polysulphone molecular weight on the membrane properties, J. Membr. Sci., 455 (2014) 187–199.
[15] S.S. Ray, M. Okamoto, Polymer/layered silicate nanocomposites: a review from preparation to processing, Prog. Polym. Sci., 28 (2003) 1539–1641.
[16] M. Ghanbari, D. Emadzadeh, W.J. Lau, T. Matsuura, M. Davoody, A.F. Ismail, Super hydrophilic TiO_2/HNT nanocomposites as a new approach for fabrication of high performance thin film nanocomposite membranes for FO application, Desalination, 371 (2015) 104–114.
[17] G. Zeng, Z. Ye, Y. He, X. Yang, J. Ma, H. Shi, Z. Feng, Application of dopamine-modified halloysite nanotubes/PVDF blend membranes for direct dyes removal from wastewater, Chem. Eng. J., 323 (2017) 572–583.

[18] Y. Ma, F. Shi, Z. Wang, M. Wu, J. Ma, C. Gao, Preparation and characterization of PSf/clay nanocomposite membranes with PEG 400 as a pore forming additive, Desalination, 286 (2012) 131–137.
[19] X.T. Hong, Y.M. Zhou, Z.L. Ye, H.F. Zhuang, W.P. Liu, K.S. Hui, Z. Zeng, X.H. Qiu, Enhanced hydrophilicity and antibacterial activity of PVDF ultrafiltration membrane using Ag_3PO_4/TiO_2 nanocomposite against *E. coli*, Desal. Water Treat., 75 (2017) 26–33.
[20] V.K. Soni, T. Roy, S. Dhara, G. Choudhary, P.R. Sharma, R.K. Sharma, On the investigation of acid and surfactant modification of natural clay for photocatalytic water remediation, J. Mater. Sci., 53 (2018) 10095–10110.
[21] H. Lee, S.M. Dellatore, W.M. Miller, P.B. Messersmith, Mussel-inspired surface chemistry for multifunctional coatings, Science, 318 (2007) 426–430.
[22] J.H. Waite, Surface chemistry - Mussel power, Nature Mater., 7 (2008) 8–9.
[23] D.R. Dreyer, D.J. Miller, B.D. Freeman, D.R. Paul, C.W. Bielawski, Perspectives on poly(dopamine), Chem. Sci., 4 (2013) 3796–3802.
[24] L.P. Yang, S.L. Phua, J.K.H. Teo, C.L. Toh, S.K. Lau, J. Ma, X.H. Lu, A biomimetic approach to enhancing interfacial interactions: polydopamine-coated clay as reinforcement for epoxy resin, ACS Appl. Mater. Inter., 3 (2011) 3026–3032.
[25] S.L. Phua, L. Yang, C.L. Toh, S. Huang, Z. Tsakadze, S.K. Lau, Y.W. Mai, X.H. Lu, Reinforcement of polyether polyurethane with dopamine-modified clay: the role of interfacial hydrogen bonding, ACS Appl. Mater. Inter., 4 (2012) 4571–4578.
[26] S.L. Phua, L.P. Yang, C.L. Toh, G.Q. Ding, S.K. Lau, A. Dasari, X.H. Lu, Simultaneous enhancements of UV resistance and mechanical properties of polypropylene by incorporation of dopamine-modified clay, ACS Appl. Mater. Inter., 5 (2013) 1302–1309.
[27] L. Wang, L.J. Hu, S.B. Gao, D.T. Zhao, L.Q. Zhang, W.C. Wang, Bio-inspired polydopamine-coated clay and its thermo-oxidative stabilization mechanism for styrene butadiene rubber, Rsc Adv., 5 (2015) 9314–9324.
[28] Y. Cai, J.X. Li, X.W. Zhang, Y.Z. Zhang, In-situ monitoring of polysulfone membrane formation via immersion precipitation using an ultrasonic through-transmission technique, Desal. Water Treat., 32 (2011) 214–225.
[29] Y. Xuan, G. Jiang, Y. Li, J. Wang, H. Geng, Inhibiting effect of dopamine adsorption and polymerization on hydrated swelling of montmorillonite, Colloids Surfaces A: Physicochem. Eng. Asp., 422 (2013) 50–60.
[30] J. Lu, Y. Gu, Y. Chen, X. Yan, Y. Guo, W. Lang, Ultrahigh permeability of graphene-based membranes by adjusting D-spacing with poly (ethylene imine) for the separation of dye wastewater, Sep. Purif. Technol., 210 (2019) 737–745.
[31] B. Fei, B. Qian, Z. Yang, R. Wang, W.C. Liu, C.L. Mak, J.H. Xin, Coating carbon nanotubes by spontaneous oxidative polymerization of dopamine, Carbon, 46 (2008) 1795–1797.
[32] S. Weng, D. Liang, H. Qiu, Z. Liu, Z. Lin, Z. Zheng, A. Liu, W. Chen, X. Lin, A unique turn-off fluorescent strategy for sensing dopamine based on formed polydopamine (pDA) using graphene quantum dots (GQDs) as fluorescent probe, Sensors Actuators B: Chem., 221 (2015) 7–14.
[33] A.M. Slavutsky, M.A. Bertuzzi, A phenomenological and thermodynamic study of the water permeation process in corn starch/MMT films, Carbohydr. Polym., 90 (2012) 551–557.
[34] M. Zhou, Q. Liu, S. Wu, Z. Gou, X. Wu, D. Xu, Starch/chitosan films reinforced with polydopamine modified MMT: Effects of dopamine concentration, Food Hydrocolloids, 61 (2016) 678–684.
[35] A.K. Mishra, N.H. Kim, D. Jung, J.H. Lee, Enhanced mechanical properties and proton conductivity of Nafion–SPEEK–GO composite membranes for fuel cell applications, J. Membr. Sci., 458 (2014) 128–135.
[36] J. Li, X. Ni, D. Zhang, H. Zheng, J. Wang, Q. Zhang, Engineering a self-driven PVDF/PDA hybrid membranes based on membrane micro-reactor effect to achieve super-hydrophilicity, excellent antifouling properties and hemocompatibility, Appl. Surf. Sci., 444 (2018) 672–690.
[37] C. Zhao, J. Lv, X. Xu, G. Zhang, Y. Yang, F. Yang, Highly antifouling and antibacterial performance of poly (vinylidene fluoride) ultrafiltration membranes blending with copper oxide and graphene oxide nanofillers for effective wastewater treatment, J. Colloid Interface Sci., 505 (2017) 341–351.
[38] N. Meng, R.C.E. Priestley, Y. Zhang, H. Wang, X. Zhang, The effect of reduction degree of GO nanosheets on microstructure and performance of PVDF/GO hybrid membranes, J. Membr. Sci., 501 (2016) 169–178.
[39] C. Liu, L. Wu, C. Zhang, W. Chen, S. Luo, Surface hydrophilic modification of PVDF membranes by trace amounts of tannin and polyethyleneimine, Appl. Surf. Sci., 457 (2018) 695–704.
[40] S.A. McKelvey, W.J. Koros, Phase separation, vitrification, and the manifestation of macrovoids in polymeric asymmetric membranes, J. Membr. Sci., 112 (1996) 29–39.
[41] A. Qin, X. Li, X. Zhao, D. Liu, C. He, Preparation and characterization of nano-chitin whisker reinforced PVDF membrane with excellent antifouling property, J. Membr. Sci., 480 (2015) 1–10.
[42] Y. Cai, J. Li, Y. Guo, Z. Cui, Y. Zhang, In-situ monitoring of asymmetric poly(ethylene-co-vinyl alcohol) membrane formation via a phase inversion process by an ultrasonic through-transmission technique, Desalination, 283 (2011) 25–30.
[43] J. Lv, G. Zhang, H. Zhang, C. Zhao, F. Yang, Improvement of antifouling performances for modified PVDF ultrafiltration membrane with hydrophilic cellulose nanocrystal, Appl. Surf. Sci., 440 (2018) 1091–1100.
[44] H.Y. Liu, G.Q. Zhang, C.Q. Zhao, J.D. Liu, F.L. Yang, Hydraulic power and electric field combined antifouling effect of a novel conductive poly(aminoanthraquinone)/reduced graphene oxide nanohybrid blended PVDF ultrafiltration membrane, J. Mater. Chem. A, 3 (2015) 20277–20287.
[45] X. Chang, Z. Wang, S. Quan, Y. Xu, Z. Jiang, L. Shao, Exploring the synergetic effects of graphene oxide (GO) and polyvinylpyrrodione (PVP) on poly(vinylylidenefluoride) (PVDF) ultrafiltration membrane performance, Appl. Surf. Sci., 316 (2014) 537–548.
[46] W. Zhao, J. Huang, B. Fang, S. Nie, N. Yi, B. Su, H. Li, C. Zhao, Modification of polyethersulfone membrane by blending semi-interpenetrating network polymeric nanoparticles, J. Membr. Sci., 369 (2011) 258–266.
[47] C. Su, J. Chang, K. Tang, F. Gao, Y. Li, H. Cao, Novel three-dimensional superhydrophobic and strength-enhanced electrospun membranes for long-term membrane distillation, Sep. Purif. Technol., 178 (2017) 279–287.
[48] J.F. Li, Z.L. Xu, H. Yang, Microporous polyethersulfone membranes prepared under the combined precipitation conditions with non-solvent additives, Polym. Adv. Technol., 19 (2008) 251–257.
[49] D. Sun, M.-Q. Liu, J.-H. Guo, J.-Y. Zhang, B.-B. Li, D.-Y. Li, Preparation and characterization of PDMS-PVDF hydrophobic microporous membrane for membrane distillation, Desalination, 370 (2015) 63–71.
[50] R. Roshani, F. Ardeshiri, M. Peyravi, M. Jahanshahi, Highly permeable PVDF membrane with PS/ZnO nanocomposite incorporated for distillation process, RSC Adv., 8 (2018) 23499–23515.
[51] X. Zhang, L. Shen, C.-Y. Guan, C.-X. Liu, W.-Z. Lang, Y. Wang, Construction of SiO_2@MWNTs incorporated PVDF substrate for reducing internal concentration polarization in forward osmosis, J. Membr. Sci., 564 (2018) 328–341.
[52] G.Y. Zeng, Y. He, Y.Q. Zhan, L. Zhang, Y. Pan, C.L. Zhang, Z.X. Yu, Novel polyvinylidene fluoride nanofiltration membrane blended with functionalized halloysite nanotubes for dye and heavy metal ions removal, J. Hazard. Mater., 317 (2016) 60–72.
[53] M. Rezaei-DashtArzhandi, A.F. Ismail, M. Ghanbari, G. Bakeri, S.A. Hashemifard, T. Matsuura, A. Moslehyani, An investigation of temperature effects on the properties and CO_2 absorption performance of porous PVDF/montmorillonite mixed matrix membranes, J. Nat. Gas Sci. Eng., 31 (2016) 515–524.

[54] C.Y. Lai, A. Groth, S. Gray, M. Duke, Enhanced abrasion resistant PVDF/nanoclay hollow fibre composite membranes for water treatment, J. Membr. Sci., 449 (2014) 146–157.
[55] M. Rezaei, A.F. Ismail, S.A. Hashemifard, G. Bakeri, T. Matsuura, Experimental study on the performance and long-term stability of PVDF/montmorillonite hollow fiber mixed matrix membranes for CO_2 separation process, Int. J. Greenh. Gas Con., 26 (2014) 147–157.
[56] C.Y. Lai, A. Groth, S. Gray, M. Duke, Impact of casting conditions on PVDF/nanoclay nanocomposite membrane properties, Chem. Eng. J., 267 (2015) 73–85.